

2012

# Charge Reduction Potentials of Several Refrigerants Based on Experimentally Validated Micro-Channel Heat Exchangers Performance and Charge Model

Yadira Padilla Fuentes  
ypadill2@uiuc.edu

Predrag S. Hrnjak

Follow this and additional works at: <http://docs.lib.purdue.edu/iracc>

---

Padilla Fuentes, Yadira and Hrnjak, Predrag S., "Charge Reduction Potentials of Several Refrigerants Based on Experimentally Validated Micro-Channel Heat Exchangers Performance and Charge Model" (2012). *International Refrigeration and Air Conditioning Conference*. Paper 1241.  
<http://docs.lib.purdue.edu/iracc/1241>

This document has been made available through Purdue e-Pubs, a service of the Purdue University Libraries. Please contact [epubs@purdue.edu](mailto:epubs@purdue.edu) for additional information.

Complete proceedings may be acquired in print and on CD-ROM directly from the Ray W. Herrick Laboratories at <https://engineering.purdue.edu/Herrick/Events/orderlit.html>

# Charge Reduction Potentials of Several Refrigerants Based on Experimentally Validated Micro-Channel Heat Exchangers Performance and Charge Model

Yadira PADILLA FUENTES<sup>1</sup> and Pega HRNJAK<sup>2\*</sup>

<sup>1</sup>Department of Mechanical Science and Engineering, University of Illinois at Urbana-Champaign  
1206 West Green Street, Urbana, IL 61801, USA  
Contact Information ([ypadill2@illinois.edu](mailto:ypadill2@illinois.edu))

<sup>2</sup>CTS – Creative Thermal Solutions  
Urbana, IL, 61801, USA  
Contact Information ([pega@illinois.edu](mailto:pega@illinois.edu))

\* Corresponding Author

## ABSTRACT

This paper presents an experimentally validated simulation model developed to obtain accurate prediction of evaporator microchannel heat exchanger performance and charge. Effects of using various correlations are presented and discussed with focus on serpentine microchannel evaporators. Experiments with propane are used to validate the model. The experimentally validated model is used to compare the charge reduction potential of various refrigerants. The procedure for charge reduction analysis described in the paper is the reduction of the internal (refrigerant) volume of the evaporator until an evaporator pressure drop is obtained that results in a 2% decrease in COP from the refrigeration cycle with no pressure drop.

## 1. INTRODUCTION

It is clear that charge reduction is beneficial for any refrigerant in any application. For HFC's and HCFC's with non-negligible GWP, charge reduction decreases the carbon footprint caused by direct refrigerant emissions. Charge reduction also makes economic sense when using more costly, synthetic low-GPW refrigerant alternatives. Even for natural refrigerants, charge reduction is desirable, especially for working fluids possessing unwanted characteristics (flammability, material incompatibility, toxicity) (Hoehne and Hrnjak, 2004). Significant charge reduction, specifically below 50 g of total charge in the refrigeration system, might open some doors for application of these hydrocarbon refrigerant systems in the USA. Very low charge NH<sub>3</sub> (R717) systems may find use in chillers for application in populated areas (Hrnjak, 2005, 2010). More reliable and accurate prediction tools are needed that allow engineers to design low-charge systems and components without sacrificing capacity and energy efficiency.

## 2. EVAPORATOR MODELING

### 2.1 Model Description

The evaporator model is based on the finite volume approach. The model was built for serpentine heat exchangers. For a serpentine design, the evaporator is divided into 60 elements along the length of the refrigerant tube for each tube pass. Inlet conditions of the fluids and geometric parameters of the heat exchanger are provided to the evaporator model. The effectiveness-NTU ( $\epsilon$ -NTU) method and pertinent correlations are used to calculate the heat transfer, pressure drop, and refrigerant charge in each element. The outlet of each element is used as the inlet to the next element.

The air velocity and air temperature profiles are assumed uniform for the evaporator model. Transition regions near saturation lines are incorporated to reduce singularities caused by correlations or data processing in the program.

The evaporator model is implemented in Engineering Equation Solver (EES, 2011). The model shows in detail the progress of the refrigerant through each element of the heat exchanger.

The air side heat transfer correlations examined in the heat exchanger model were by Sunden and Svantesson (1992), Chang and Wang (1997), Kim and Bullard (2002), Park and Jacobi (2009), and Li and Wang (2010).

In refrigerant side single phase regions, Churchill's (1977) friction factor correlation was used to calculate the friction factor for the pressure drop across the element while the Dittus-Bolter (1930) correlation was used to find the single phase refrigerant side heat transfer coefficient. For void fraction, in addition to the homogeneous assumption, correlations by Zivi (1964), Armand (1946), Butterworth (1974), Steiner (1993), Graham et. al. (1997), Graham et. al. (1999), Yashar et. al. (2001), Niño et. al. (2002), Jassim et. al. (2006), (2008), and Shedd (2010) were examined.

In order to calculate the refrigerant mass in the heat exchanger, the void fraction was calculated in each element. The total mass is calculated using Equation 1 where  $M$  is the refrigerant mass in the element in the two phase region,  $\alpha$  is the void fraction,  $A_{cs}$  is the refrigerant cross sectional area,  $L_{element}$  is the length of the element, and  $\rho_{vapor}$  and  $\rho_{liquid}$  are the vapor and liquid densities in the element respectively. Fig. 1 shows the charge in each element as you move along the circuiting length for the serpentine evaporator (Traeger and Hrnjak, 2005). The masses calculated in each element are summed to obtain the total mass in the evaporator. The area under the curve shown in Fig. 1 represents the summation of these elements. The figure shows that the majority of the charge is found in the two-phase region (where area is the largest). This is the reason why there is an emphasis on accurate modeling of the two-phase region correlations (Hrnjak, 2002).

$$M = \sum_1^n A_{cs} L_{element} (\alpha \rho_{vapor} + (1 - \alpha) \rho_{liquid}) \quad (1)$$

Correlations by Chen (1966), Gungor and Winterton (1986), Liu and Garimella (2007), and Pamitran et. al. (2009) were considered for two-phase refrigerant heat transfer coefficient. For evaporation two phase pressure drop, correlations by Friedel (1979), Müller-Steinhagen and Heck (1986), Souza and Mattos Pimenta (1995), Mishima and Hibiki (1996), Zhang and Webb (2001), Niño et. al. (2002), Lee and Mudawar (2005), and English and Klandikar (2006) were examined.

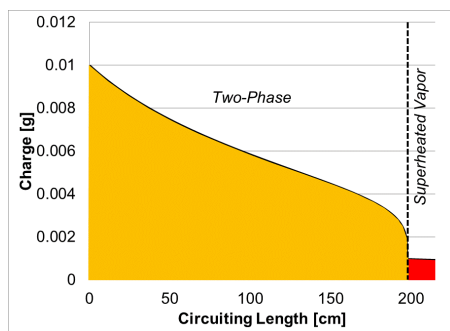


**Figure 1:** Charge distribution along serpentine evaporator with R290 from Traeger and Hrnjak (2005) shown in Fig. 3

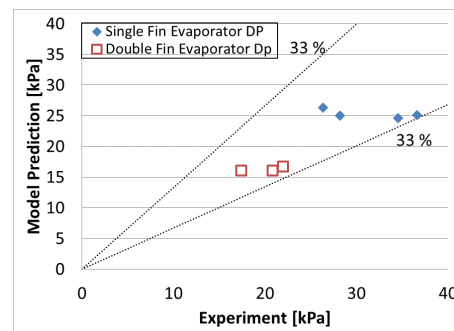


**Figure 2:** Souza and Mattos Pimenta (1995) correlation predicts R290 evaporators  $\Delta P$  data within 33 %

## 2.2 Model Validation

Experimental data from the Air Conditioning and Refrigeration Center (ACRC) at the University of Illinois at Urbana-Champaign was used to validate the model; data from Traeger and Hrnjak (2005) for a 1 kW serpentine R290 (propane) evaporators was the primary model validation source, specifically for refrigerant charge. Two types of evaporators were used, one with single fin between tubes (Fig. 3) and one with two fin heights between tubes (Fig. 4). The face area is roughly the same for both evaporators.

For pressure drop in the two-phase region, it was found that correlations by Souza and Mattos Pimenta (1995), followed by Mudawar (2005), and then Friedel (1979) predicted the data well. All other pressure drop correlations deviated more than 33% from experimental results for both evaporators. By using Souza and Mattos Pimenta (1995) the pressure drop was predicted with  $\pm 33\%$ , shown in Fig. 2.

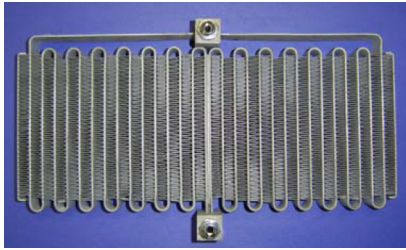


**Figure 3:** Single fin serpentine design evaporator from Hrnjak and Traeger (2005)

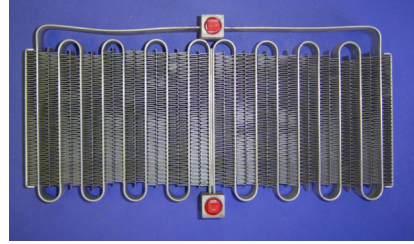


**Figure 4:** Double fin serpentine design evaporator from Hrnjak and Traeger (2005)

For refrigerant heat transfer coefficient, Pamitran et. al. (2009), Chen (1966), and Gungor and Winterton (1986) compared favorably to experimental results. The Garimella (2007) correlation for heat transfer coefficient was not a good predictor of refrigerant heat transfer coefficient for the evaporators with errors of  $\pm 30\%$  for the single finned evaporator (Fig. 3) and  $\pm 40\%$  for the doubled finned evaporator (Fig. 4).

For the evaporator with one fin height, the best agreement for air side heat transfer to experimental data was provided by Park and Jacobi (2009), followed by Kim and Bullard (2002), and then Chang and Wang (1997). All other correlations resulted in over-predicted superheat for the single fin evaporator. By using Pamitran et. al. (2009) for refrigerant heat transfer coefficient and Park and Jacobi (2009) for air side heat transfer coefficient,

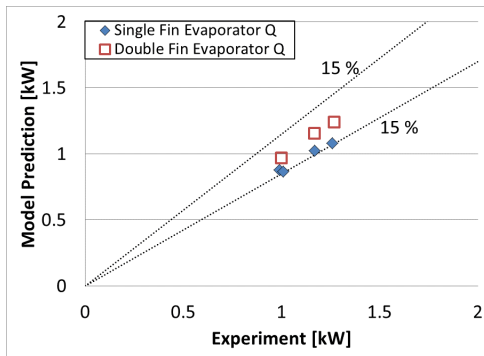


**Figure 5:** Capacity of serpentine evaporators using Pamitran et. al. (2009) and Park and Jacobi (2009)

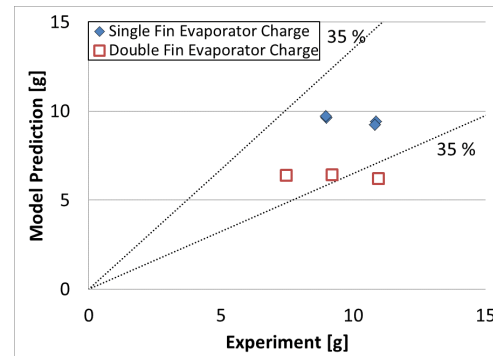


**Figure 6:** Charge prediction of serpentine evaporators using Graham (1997) void fraction correlation

the capacity was predicted within  $\pm 15\%$  from experimental values for both evaporator designs shown in Fig. 5.

Charge prediction was better for the single fin design with lowest error of  $-12\%$  and highest error of  $+9\%$  from experimental results. Charge prediction for both evaporator designs is shown in Fig. 6. Superheat and charge were not accurately predicted for the two fin evaporator in Fig. 4. The best results were attained using the described correlations for the single fin evaporator in Fig. 3. Therefore analysis to be presented will be calculated by using a single fin design evaporator.

### 3. EXAMPLE: POTENTIAL FOR CHARGE REDUCTION

#### 3.1 Potential for Charge Reduction

The model developed and validated above was used to evaluate the charge minimization potential of several refrigerants in the serpentine evaporator. The procedure is described below.

#### 3.2 The Conceptual Framework

It is assumed that the fair comparison of the charge reduction potential of refrigerants requires maintaining the same geometry and capacity of the system while exposing the evaporator to the same conditions on the air side (air side

velocity, inlet temperature, etc.) when analyzing each working fluid (Hrnjak, 2009). Additionally, the effect of the evaporator on the rest of the refrigerant side of the system should be the same and is here defined as a 2 % difference between COP's of the system with a real evaporator with pressure drop and ideal evaporator without pressure drop on the refrigerant side.

When the same heat exchanger is redesigned for different refrigerants, internal volume is adjusted to the minimal value that creates a pressure drop which causes a 2% drop in COP. Internal volume minimization is chosen to be representative of charge minimization even though some other effects like changes in mass flux may occur (Hrnjak, 2010). For that reason, the heat exchanger design selected is a microchannel, serpentine (single pass) evaporator with a constant number of ports, shown in the Fig. 9. Furthermore, Hrnjak and Litch 2001 showed that the serpentine design had the least refrigerant charge while maintain similar capacity as single pass and two pass condensers of similar size with ammonia as the working fluid. The serpentine design is selected to avoid uncertainties in prediction of refrigerant charge in the headers. The authors believe that this design does not affect the generality of conclusions.

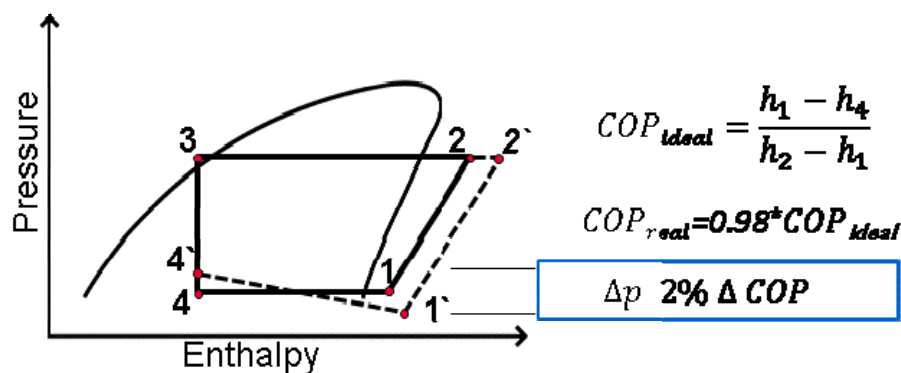


**Figure 7:** Comparison criteria for microchannel heat exchangers based on pressure drop that causes 2% change in COP

As stated earlier, for each refrigerant, heat exchanger air side geometry is identical; outer dimensions of the tube, length of the tube, and number of ports (channels) are constant and identical. Modifications are made to the diameter of the ports that generate the same degradation of COP due to refrigerant side pressure drop compared to the case without pressure drop (ideal) while maintaining the same system cooling capacity.

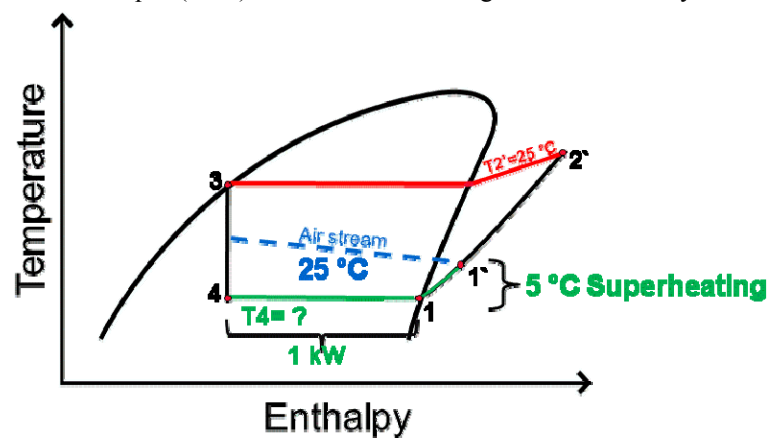


**Figure 8:** Air side and refrigerant side operating conditions for this example

The other similar option is to vary the number of active ports as needed but keep the diameter of the ports constant without varying the outer dimensions of the flat tube.

Fig. 7 shows the “ideal”, baseline cycle, in solid line and the “real”, actual cycle, with the dashed line. The pressure drop in real evaporator causes a 2% reduction in COP compared to the “ideal” cycle. The cooling capacity and the LMTD for the “ideal” and “real” cycle are the same. Isenthalpic expansion and isentropic compression are assumed in both cycles for all fluids. This assumption does not affect the generality of conclusions.

The example shown below is for an operating condition with dry air, air inlet temperature into evaporator of 25 °C, and face velocity of 2.5 m/s.

**Table 1:** Geometry inputs for this example

| Fins                              |       | Tubes                   |        | Overall                       |        |
|-----------------------------------|-------|-------------------------|--------|-------------------------------|--------|
| Fin height [mm]                   | 8     | Number of MC tubes [-]  | 2      | Width [mm]                    | 115    |
| Fin depth [mm]                    | 35    | Tube thickness [mm]     | 2.3    | Height [mm]                   | 206    |
| Fin thickness [mm]                | 0.15  | Tube depth [mm]         | 35     | Depth [mm]                    | 35     |
| Fins per inch [in <sup>-1</sup> ] | 15    | Number of ports [-]     | 20     | Circuits [-]                  | 2      |
| Fin Pitch [mm]                    | 1.693 | Hydraulic diameter [mm] | Varies | Runs per Circuit [-]          | 10     |
| Louver height [mm]                | 7.2   | Absolute roughness [mm] | 0.0015 | Air HT area [m <sup>2</sup> ] | 0.9136 |
| Louver pitch [mm]                 | 1.72  |                         |        |                               |        |
| Louver angle [°]                  | 27    |                         |        |                               |        |

The evaporation temperature is around 0 °C. The predicted results are provided for each fluid in Table 2. Cooling capacity of the evaporator is 1 kW and superheat at the exit is 5 °C above saturation. The condensing temperature is set to 25 °C. The outlet of the condenser is assumed saturated (quality of zero) and no pressure drop is assumed in the condenser. Cycle operating conditions are shown in Fig. 8, and geometric parameters are given in Table 1 and Fig. 9.

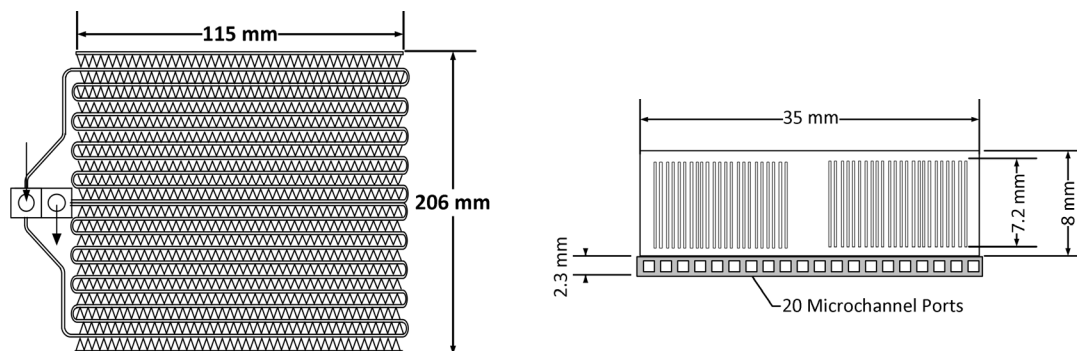


**Figure 9:** Baseline serpentine condenser design

### 3.3 Analysis Procedure

Fig. 10 shows the logic flow diagram implemented in order to analyze the charge potential of the refrigerants. The below steps describe the iterative procedure shown in the figure.

1. First for the given conditions and geometry, guess an evaporator inlet saturation temperature ( $T_{esati}$ ), refrigerant mass flow rate ( $\dot{m}_r$ ), and hydraulic diameter ( $D_h$ ). These values are inserted into the ideal cycle to get out the pressure ( $P_{eri}$ ), temperature ( $T_{eri}$ ), and quality ( $x_{eri}$ ) into the real evaporator model.

- The real evaporator model outputs capacity ( $Q_{\text{evap}}$ ), which is checked to see if it is 1 kW. If this condition is not met, then the saturation temperature is changed by some amount ( $\Delta_1$ ) and the process is repeated from step 1 until cooling capacity is 1 kW.
- Once cooling capacity is 1 kW, a check is made to see if the superheat temperature ( $T_{\text{sup}}$ ) of the evaporator is 5 °C. If it does not, the mass flow rate is changed and the procedure is repeated from step 1 until superheat temperature is 5 °C and previous steps are satisfied.
- Once steps 2 and 3 are completed, the ideal cycle is run again using the logarithmic mean temperature difference of the real cycle ( $\text{Lmtd}_{\text{real}}$ ) as the logarithmic mean temperature difference of the ideal cycle ( $\text{Lmtd}_{\text{ideal}}$ ). The ideal cycle is set to have 5 °C superheat and 1 kW cooling capacity (the difference in COP comes from the differences in work in both cycles). The  $\text{COP}_{\text{ideal}}$  and  $\text{COP}_{\text{real}}$  are calculated for the cycles and compared so that the ratio of  $\text{COP}_{\text{ideal}}$  to  $\text{COP}_{\text{real}}$  is 1.02.
- If the ratio is not 1.02 then the hydraulic diameter is changed by some amount ( $\Delta_3$ ), and the procedure is repeated from step 1 until steps 2, 3 and 4 are satisfied.
- Once the ratio is 1.02, then the analysis for that refrigerant is completed. The process is repeated for each new refrigerant using the same heat exchanger. The results are shown in Table 2.

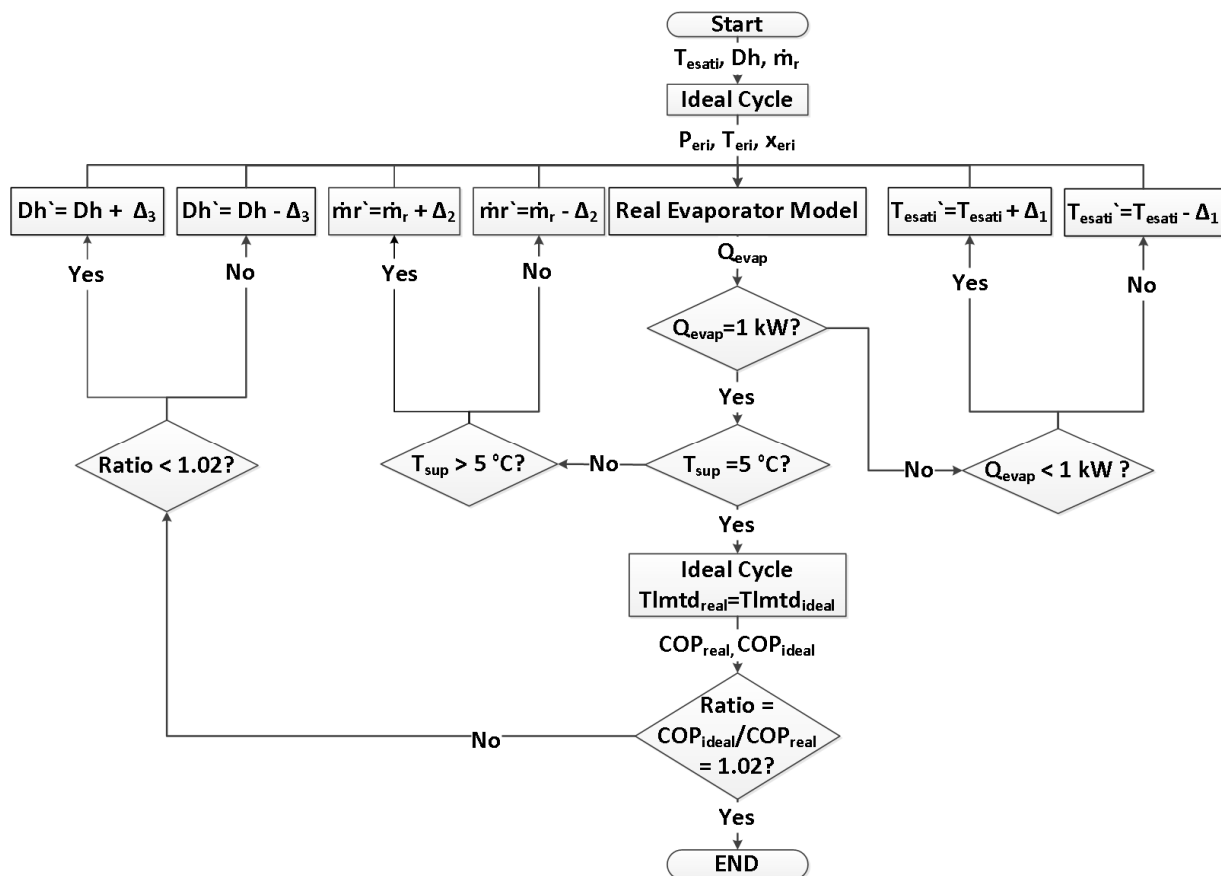


**Figure 10:** Logic flow diagram used to obtain 2% COP decrease due to pressure drop

### 3.4 Results

For each refrigerant, the pressure drop needed to reduce the COP by 2 % was calculated and is listed in Table 2. Table 2 also shows the amount of charge in the evaporator for each refrigerant. Fig. 9 is a schematic of this data with the needed hydraulic diameter to reduce the COP by 2%.

**Table 2:** Refrigerant charges in evaluated evaporator based on pressure drop that causes 2% COP reduction compared to idealized ( $\Delta P=0$  cycle with equal LMTD)

| Fluid   | Ref. Mass | Hydraulic Diameter | Mass Flow Rate | $\Delta P$ [2 % COP reduction] | COP Ideal | Evap. Temperature | Sat. Liquid Density  | Sat. Vapor Density   | Latent Heat |
|---------|-----------|--------------------|----------------|--------------------------------|-----------|-------------------|----------------------|----------------------|-------------|
|         | [g]       | [mm]               | [g/s]          | [kPa]                          | [-]       | [°C]              | [kg/m <sup>3</sup> ] | [kg/m <sup>3</sup> ] | [kJ/kg]     |
| R134a   | 23.16     | 1.420              | 5.962          | 15.30                          | 9.217     | 0.051             | 1295.0               | 13.7                 | 197.8       |
| R1234yf | 18.85     | 1.380              | 7.540          | 15.83                          | 8.947     | -0.018            | 1176.0               | 16.8                 | 162.4       |
| R600a   | 16.44     | 1.810              | 3.310          | 8.13                           | 9.336     | -0.0253           | 580.3                | 4.1                  | 352.8       |
| R410A   | 6.51      | 0.820              | 5.340          | 40.31                          | 8.825     | 0.007             | 1176.0               | 29.2                 | 222.6       |
| R717    | 5.38      | 1.000              | 0.864          | 26.06                          | 9.361     | 0.357             | 638.2                | 3.3                  | 1259.0      |
| R32     | 5.34      | 0.785              | 3.631          | 40.98                          | 8.911     | 0.188             | 1055.0               | 21.1                 | 314.7       |
| R290    | 4.24      | 1.010              | 3.164          | 22.30                          | 9.044     | -0.024            | 528.3                | 9.9                  | 372.8       |
| R744    | 2.49      | 0.498              | 6.060          | 152.40                         | 6.396     | 0.363             | 925.2                | 93.8                 | 230.7       |

R744 shows the highest potential for charge reduction when using the 2% change in COP criterion for pressure drop. Highest potential means that for the same capacity, the same air side conditions and geometry, and the same 2% COP reduction due to pressure drop, the amount of charge is the smallest with the least internal volume. This means that the refrigerant with highest charge reduction can provide the same performance as other fluids but with the least amount of charge.

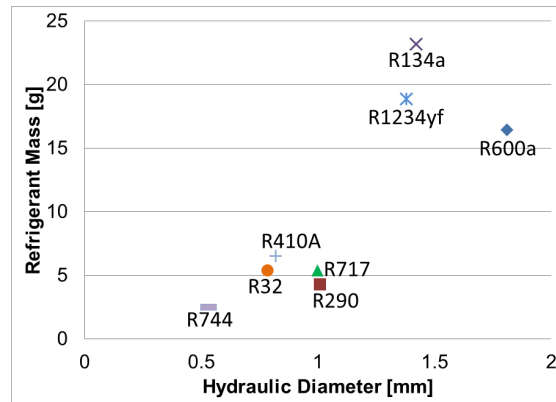


**Figure 11:** Refrigerant charge (Mass) and hydraulic diameter of serpentine evaporator for 1kW refrigeration system causing 2% difference from ideal COP due to evaporator pressure drop

Carbon dioxide (R744) owes its high charge reduction potential to low pressure drop (due to dense vapor) and low sensitivity to pressure drop, as shown in Table 2, column 5,  $\Delta P$  [2 % COP reduction]. This means that high pressure drop will not result in high temperature drop of the fluid (which affects the COP). This small change in temperature, due to high pressure drop, tells us that the COP is not affected significantly if the pressure drop is high. This is an

advantage for R744 since it means that it can perform well in microchannel heat exchangers. Once internal volume is defined, dense vapor at any void fraction will give higher refrigerant mass which is a disadvantage to R744. Even though hydraulic diameter is the largest for R600a (Isobutane), the highest charge is predicted for R134a and R1234yf due to their higher sensitivity to pressure drop and relatively high densities. Isobutane is not ranked as the highest because it has lower vapor and liquid densities than R1234yf and R134a.

#### 4. SUMMARY AND CONCLUSIONS

This paper presented an experimentally validated model of an air cooled microchannel evaporator, focused on refrigeration capacity, pressure drop, and charge reduction. The following correlations showed the best agreement with experimental results:

- Air side heat transfer and pressure drop: Park and Jacobi (2009)
- Refrigerant side heat transfer and pressure drop: Pamitran et. al. (2009) and Souza and Mattos Pimenta (1995)
- Refrigerant charge inventory: Graham (1997)

An example of utilizing the model for evaluation of refrigerant charge potential of various refrigerants is presented. The criterion for evaluation was reduction in internal volume until refrigerant side pressure drop caused 2% COP reduction over the zero pressure drop case. For each refrigerant evaluated, all conditions and dimensions on the air side of the heat exchanger were maintained identically; only the hydraulic diameter of the port (channel) was allowed to be changed.

Results show that R744 has the highest potential for charge reduction, followed by R32. R744 requires mass flow rate similar to other refrigerants but its dense vapor reduces velocity and thus refrigerant side pressure drop, and assisted with low cycle sensitivity to pressure drop.

#### NOMENCLATURE

|                    |  |                      |
|--------------------|--|----------------------|
| $A_{cs}$           | cross sectional area                                       | (m <sup>2</sup> )    |
| $\alpha$           | void fraction  | (-)                  |
| $COP_{ideal}$      | coefficient of performance ideal cycle                     | (-)                  |
| $COP_{real}$       | coefficient of performance modeled cycle                   | (-)                  |
| $D_h$              | hydraulic diameter   | (m)                  |
| $D_h'$             | new hydraulic diameter                                     | (m)                  |
| $\Delta_1$         | small change in temperature                                | (°C)                 |
| $\Delta_2$         | small change in port diameter                              | (m)                  |
| $\Delta_3$         | small change in ref. mass flow rate                        | (m)                  |
| $h$                | enthalpy   | (kJ/kg)              |
| $L_{element}$      | length of element section                                  | (m)                  |
| $M$                | total charge   | (g)                  |
| $\dot{m}_r$        | refrigerant mass flow rate                                 | (kg/s)               |
| $P_{eri}$          | inlet refrigerant pressure                                 | (kPa)                |
| $Q_{evap}$         | evaporation capacity                                       | (kW)                 |
| $\rho_{liquid}$    | density of liquid  | (kg/m <sup>3</sup> ) |
| $\rho_{vapor}$     | density of vapor   | (kg/m <sup>3</sup> ) |
| $T_{esati}$        | condensation saturation temperature                        | (°C)                 |
| $T_{esati}'$       | new condensation saturation temperature                    | (°C)                 |
| $T_{eri}$          | inlet refrigerant temperature                              | (°C)                 |
| $l_{lmtd_{ideal}}$ | logarithmic mean temperature difference of the ideal cycle | (°C)                 |
| $l_{lmtd_{real}}$  | logarithmic mean temperature difference of the real cycle  | (°C)                 |
| $LMTD$             | logarithmic mean temperature difference                    | (°C)                 |
| $T_{sup}$          | superheat temperature                                      | (°C)                 |
| $x_{eri}$          | quality at outlet of condenser                             | (-)                  |

## REFERENCES

- Armand, A.A., 1946, The Resistance during the Movement of a Two-Phase System in Horizontal Pipes, *Izv. Vses. Teplotekh. Inst.* 1, 16–23.
- Butterworth D., 1974, An analysis of film flow and its application to condensation in a horizontal tube, *Int. J. Multiphase flow*, Vol 1, 671-682
- Chang Y.J., Wang C.C., 1997, A generalized heat transfer correlation for louver fin geometry, *Int. J. Heat Mass Transsfer*, Vol 40 (5), 533-544
- Chen J.C., Correlation for boiling heat transfer to saturated fluids in convective flow, 1966, A.I.Ch.E.-A.S.M.E. Heat Transfer Conference, ASME paper 63-HT-34, 322-329
- Churchill S.W., Usagi R., 1972, A General Expression for the Correlation Rates of Transfer and Other Phenomena, *AIChE J.*, Vol. 18 (6) November 1972
- Dittus, P. W., Boelter L. M. K., 1930, *Univ. Calif. Pub. Eng.*, Vol. 2, no. 13, 443-461, Reprinted in *int. Comm. Heat mass transfer*, vol. 12, Pp. 3-22 (1985)
- Engineering Equation Solver-Academic Professional V8.874, 2011, F-Chart Software, Middleton, WI.
- English N.J., Kandlikar S.G., 2006, An experimental investigation into the effect of surfactants on air-water two-phase flow in minichannels, *Heat transfer engineering*, 27 (4), 99-109
- Friedel L., 1979, Improved friction pressure drop correlations for horizontal and vertical two phase pipe flow, *3R International*, 18 Jahrgang, Heft 7, 485-491
- Graham D.M., Newell T.A., Chato J.C. 1997, Experimental investigation of void fraction during refrigerant condensation, *Air Condition and Refrigeration Center*, University of Illinois, Technical Report 135
- Graham D.M., Kopke H.R., Wilson M.J., Yashar D.A., Chato J.C., Newell T.A., 1999, An investigation of void fraction in the stratified/annular flow regions in smooth, horizontal tubes, *Air Condition and Refrigeration Center*, University of Illinois, Technical Report 144
- Gungor K.E., Winterton R.H.S., 1986, A general correlation for flow boiling in tubes and annuli, *Int. J. Heat Mass Transfer*, Vol. 29 (3), 351-358
- Hrnjak, P. S. and A. D. Litch, 2001, Charge Reduction in Ammonia Chiller Using Air-Cooled Condensers with Aluminum Microchannel Tubes, *Proc. of IIR*, Long Beach, CA, 235-267
- Hrnjak, P. S., 2002 Microchannel Heat Exchangers as a Design Option for Charge Minimization on NH<sub>3</sub> and HC Systems, *Proc. of IIR Conference Zero Leakage - Minimal Charge*, Stockholm, 111-118
- Hoehne, M. and P. S. Hrnjak, 2004, Charge Minimization in Hydrocarbon Systems, *Proc. of the IIR Conference*, Gustav Lorentzen in Glasgow
- Hrnjak, P. S., 2005, "Charge Reduction in Ammonia Systems," Keynote Lecture, *IIR Conference*, Ohrid
- Hrnjak, P. S. 2009, Refrigerant Charge Reduction: Strategies and Experience, *IIR 1st Workshop on Refrigerant Charge Reduction*, Cemagref Antony, France
- Hrnjak, P., 2010, "Ultra Low Charged Air Cooled Ammonia Chillers," 9th *IIR Gustav Lorentzen Conference on Natural Working Fluids*, Sydney, April 12-14
- Hrnjak, P.S., 2010, "Developments in Charge Reduction and Microchannel Technology-Mass Flux as a Way to Affect Void Fraction.Charge," 2nd *IIR Workshop on Refrigerant Charge Reduction*, KTH, Stockholm, June 16-17, 2010.
- Jassim E.W., Newell T.A., Chato J.C., 2006, Probabilistic flow regime map modeling of two phase flow, *Air Condition and Refrigeration Center*, University of Illinois, Technical Report 248
- Jassim E.W., Newell T.A., Newell B.E., 2010, Prediction of two-phase heat transfer in horizontal multi-port microchannels using probabilistic flow regime maps, *Air Condition and Refrigeration Center*, University of Illinois, Technical Report 274
- Kim M.H., Bullard C.W., 2002, Air-side thermal hydraulic performance of multi-louvered fin aluminum heat exchangers, *Int. J. of Refrigeration*, 25, 390-400
- Lee J., Mudawar I., 2005, Two phase flow in high-heat-flux micro-channel heat sink for refrigeration cooling applications: Part II-Heat transfer characteristics, *Int. J. of Heat and Mass Transfer*, 48, 941-955
- Li W., Wang X., 2010, Heat transfer and pressure drop correlations for compact heat exchangers with multi-region louver fins, *Int. J. of Heat and Mass Transfer*, 53, 2955-5962
- Liu D., Garimella S.V., 2007, Flow in boiling heat transfer in microchannels, *J. of Heat Transfer*, Vol. 129, 1321-1332
- Mishima K., Hibiki., 1996, Some characteristics of air-water two-phase flow in small diameter vertical tubes, *Int. J. Multiphase Flow*, Vol 22 (4), 703-712
- Müller-Steinhagen H., Heck K., 1986, A simple friction pressure drop correlation for two-phase flow in pipes, *Chem. Eng. Process*, 20, 297-308
- Niño V.G., Hrnjak P.S., Newell T.A., 2002, Characterization of two-phase flow in microchannels, *Air Condition and Refrigeration Center*, University of Illinois, Technical Report 202
- Pamitran A.S., Choi K.I., Oh J.T., Park K.Q.W., 2009, Two-phase heat transfer of propane vaporization in horizontal minichannels, *J. of Mechanical Science and Technology*, (23), 599-606
- Park Y.G., Jacobi A.M., 2009, Air-side heat transfer and friction correlation for flat-tube louver-fin heat

- exchangers, *J. Heat Transfer*, Vol. 131 (February), 021801-1 to 021801-12
- Shedd T.A., 2010, Void fraction and pressure drop measurements for refrigerant R410A flows in small diameter tubes, Multiphase Visualization and Analysis Laboratory, University of Wisconsin-Madison, Final report presented to AHRI
- Steiner, D., 1993, Heat Transfer to Boiling Saturated Liquids” VDI-Wärmeatlas (VDI Heat Atlas), Verein Deutscher Ingenieure, VDI-Gesellschaft Verfahrenstechnik und Chemieingenieurwesen (GCV), Düsseldorf, Chapter Hbb
- Souza A.L., Mattos Pimenta M., 1995, Prediction of pressure drop during horizontal two-phase flow of pure and mixed refrigerants, *Cavitation and Multiphase flow*, Vol. 210, 161-171
- Sunden B., Svantesson J., 1992, Correlation of  $j$ - and factors for multilouvered heat transfer surfaces, *Proceedings of the 3rd UK National Heat Transfer ConS*, pp.805-811
- Traeger K.M., Hrnjak P.S., 2005, Charge minimization of microchannel heat exchangers, Air Condition and Refrigeration Center, University of Illinois, Technical Report 251
- Yashar D.A., Wilson M.J., Kopke H.R., Graham D.M., Chato J.C., Newell T.A., 2001, An Investigation of refrigerant void fraction in horizontal, microfin tubes, *HVAC&R Research*, 7 (1), 67-82
- Zhang M., Webb R.L., 2001, Correlation of two-phase friction for refrigerants in small-diameter tubes, *Experimental Thermal and Fluid Science*, 25, 131-139
- Zivi S.M., 1964, Estimation of steady-state steam void fraction by means of the principle of minimum entropy production, *J. Heat Transfer*, 86 *Trans. Am. Soc. Mech. Engrs, Series C* (1964), 247–252.

## 7. ACKNOWLEDGEMENTS

Authors are grateful for funding support to all member companies of the Air Conditioning and Refrigeration Center at the University of Illinois at Urbana Champaign.